Shear alignment of confined hydrocarbon liquid films

Carlos Drummond,[1] Norma Alcantar,[2] and Jacob Israelachvili[2]
[1]*INTEVEP, S. A. Apdo 76343, Caracas 1070-A, Venezuela*
[2]*Department of Chemical Engineering, and Materials Department, University of California, Santa Barbara, California 93106*
(Received 19 February 2002; published 26 July 2002)

Shear-induced structural reordering in thin liquid films of the linear saturated alkane *n*-eicosane ($C_{20}H_{42}$) was investigated using a surface forces apparatus and freeze-fracture (atomic force) microscopy (AFM). By rapidly freezing a shearing film followed by splitting (cleaving) the films from the confining mica substrate surfaces, it was possible to obtain AFM images of the structures of the films during steady-state sliding, revealing striped domains $\approx$2 Å in height and a few nanometer wide whose structure depends on the sliding velocity and, most likely, also on the sliding distance and time. In contrast, confined but unsheared films yielded completely featureless images. To the best of our knowledge, the results are the first direct experimental measurement of shear-induced ordering in nano-confined films resulting in layering and domain formation, but any molecular-level alignment, if present, could not be established.

DOI: 10.1103/PhysRevE.66.011705 PACS number(s): 61.30.Hn, 62.40.+i, 68.08.De, 68.37.Ps

I. INTRODUCTION

Linear and branched hydrocarbons (alkanes) have long been the major components of oil-based lubricant fluids or ''lube oils.'' Yet in spite of their structural simplicity, a complete understanding of the relationship between molecular structure and their nanoscale and microscale behavior when trapped between two shearing surfaces (i.e., their lubricity or thin-film rheology) is still lacking.

During the last decade, the introduction of new experimental techniques and more powerful computers and models have lead to a renewal of research and a greatly increased understanding of this subject. In nonequilibrium molecular dynamics simulations, Berker and co-workers [1] observed strong molecular alignment along the shearing direction in bulk liquid *n*-hexadecane at shear rates higher than 10^{10} s^{-1}; they also observed a deviation from the static spherical distribution at lower shear rates. Cui and co-workers [2] observed a similar behavior in rheological modeling of several linear hydrocarbons. They reported a monotonic reduction of the alignment angle of the molecules with increasing shear rate, from the static equilibrium value of 45° to less than 10° at the highest shear rates investigated. Kioupis and Maginn [3] used the same simulation techniques to investigate mixtures of *n*-hexane and *n*-hexadecane and observed the same behavior: strong shear alignment of the molecules along the flow direction at shear rates higher than 10^{9} s^{-1}. Using the same techniques, Moore and co-workers [4] reported shear-induced ordering in a liquid composed of hydrocarbon chains of 100 carbon atoms ($C_{100}H_{202}$) with a limiting alignment angle of 2°–3° for strains larger than ten and shear rates above 10^{9} s^{-1}. All these simulations modeled flow in bulk (not confined) liquids.

In spite of the many *theoretical* predictions, no *experimental* observation of shear-induced alignment in hydrocarbon chain liquids has been reported. The very high shear rates required to observe this effect are beyond the capabilities of conventional rheometers, and the transient nature of the alignment—the fluids quickly recover their disordered configuration when the shear is stopped—makes it difficult to even take a ''snapshot'' of this phenomenon. Yet high shear rates, of the order 10^{8} s^{-1}, are routinely achieved in lubricated disk drives, micromachines, and automobile engines. In contrast, structural changes during bulk shear of more complex fluids have been observed many times by *in situ* scattering studies using x rays [5], neutrons [6,7], and light [8] of a variety of systems including liquid crystals [9], polymer melts [10], and emulsions [11]. In general, these low-shear-rate studies have shown that macromolecules and soft fluid microstructures align parallel to or become deformed (elongated) along the direction of flow, this effect being accompanied by a shear thinning (reduced viscosity) of the fluid.

Even more challenging, but of great practical importance, is the dynamic behavior of fluids under confinement, which arises in thin films during lubricated sliding and in the flow of fluids through small pores or capillaries (strictly, the three examples given above belong to this category). There are increased difficulties associated with measuring molecular orientation in highly confined geometries using scattering probes because of the great reduction in sample size. The x-ray surface forces apparatus [12,13] has been successfully used for studying shear-induced ordering in several *mesoscopic* films, but its application to thinner films awaits the successful use of stronger x-ray sources. Soga and co-workers [14] used time-resolved infrared spectroscopy to study the behavior of liquid crystal films of thickness of 10 μm under shear; and recently, Kuhl and co-workers [15] reported the design of a new ''confinement and shear cell'' for studying structure in films thinner than 0.1 μm. However, to our knowledge, no direct experimental data of shear alignment in nanoscale confined films has been reported.

On the simulation side, Stevens *et al.* [16] investigated a confined film of *n*-hexadecane ($C_{16}H_{34}$) under shear and found some alignment of the chains in the shear direction at the lower end of the range of sliding velocities investigated (50 m/s). Gupta, Cochran, and Cummings [17] reported strong molecular alignment in thin films of *n*-tetracosane ($C_{24}H_{50}$) at even lower sliding velocities. Khare, de Pablo, and Yethiraj [18] observed a strong tendency of connected

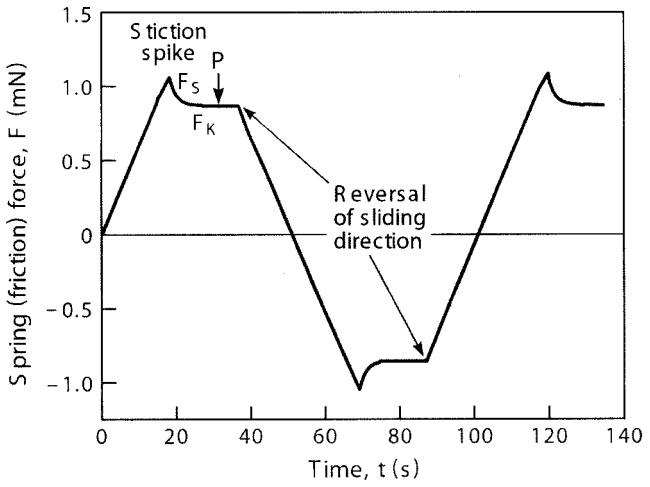

FIG. 1. Accurate reproduction of a typical friction trace showing the friction force versus time, $F(t)$, for sliding mica surfaces confining a 1.5-nm-thick film of liquid *n*-eicosane at 38°C. The sliding direction of the lower surface (and hence the sign of the measured friction force) was reversed after each traverse through a distance of $\Delta D = 28\ \mu$m. For freezing and imaging the hydrocarbon thin film, the driving of the lower surface was stopped at point *P* after 5.75 complete cycles. Other experimental parameters: sliding velocity $V = 0.5\ \mu$m/s, normal load $L = 4.0$ mN, kinetic friction force $F_k = 0.86$ mN.

chains to stretch and reorient along the flow direction. In contrast, Thompson, Robbins, and Grest [19] observed little molecular ordering in confined hydrocarbon films, and no tendency to shear align in ultrathin films at low shear rates. All these simulations lacked the time and sliding distance necessary to reach steady-state conditions. These can be of the order of many seconds and tens of microns [20], which are well beyond the range accessible by current simulations.

II. EXPERIMENT

In this paper we report results obtained by combining three well-established techniques: the surface forces apparatus (SFA) used to confine and shear liquid hydrocarbon films of nanometer thickness, freeze fracture (FF) that involves the rapid freezing of a fluid sample followed by its fracture, and atomic force microscopy (AFM) to image the fracture surface of the sheared hydrocarbon film. We investigated thin films of *n*-eicosane (Aldrich, 99%), a linear saturated alkane with a backbone of 20 carbon atoms, having a molecular length (when fully extended) of about 27 Å, a width of 3.6 Å, and a bulk melting temperature of 36 °C. An SFA-III modified for friction experiments was used for measuring the tribological properties of the films which were pressed between two molecularly smooth back-silvered mica sheets supported (glued) on cylindrical silica lenses. By passing white light normally through the uniformly flattened area of the ''contacting'' surfaces (diameter $\sim 100\ \mu$m) and examining the emerging beam with a conventional spectrometer it was possible to monitor the geometry of the contact and measure the absolute separation between the surfaces (i.e., the film thickness) with an accuracy of 2 Å. A bimorph slider [21] was used to move the lower surface laterally at some controlled constant velocity, and the shear force experienced by the upper surface (the friction force) was measured from the deflection of a vertical double cantilever spring supporting the upper surface. Further details of the friction force measuring technique have been described in the literature [22,23]. Resistor heaters were incorporated into the body of the SFA to heat the inside chamber up to 50 °C which is well above the mp of *n*-eicosane. The temperature was controlled to within 1 °C by using a PT-100 thermocouple and a closed-loop partial-integral-differential (PID) controller. A teflon injection port on the sidewall of the SFA chamber allowed injection of liquid nitrogen directly onto the contacting surfaces at any time using a hypodermic needle. This setup allowed us to quickly freeze the confined film as it was being sheared (at which point the surfaces became stuck together and stopped shearing).

After bringing two clean mica surfaces into flat contact and measuring the positions of the optical interference fringes in the spectrometer, the surface were separated by about 1 mm and a small amount of finely divided *n*-eicosane powder was placed on the lower surface and melted. The separation between the two surfaces was then reduced to $\sim 1\ \mu$m, at which separation the liquid bridge was allowed to equilibrate at 38 °C for at least 2 h. After thermal equilibration, the surfaces were brought into flattened ''contact'' under a load of $L \approx 4.0$ mN where a uniform ~ 1.5-nm-thick film of liquid eicosane remained between the two elastically deformed mica surfaces.

III. RESULTS

The film was then sheared by driving the lower surface back and forth at constant velocity V over a distance $\Delta D = 28\ \mu$m, while the friction force F was measured (recorded) as described above. A typical friction trace is presented in Fig. 1. The measured friction force is very similar to what has been previously reported for thin films of shorter linear hydrocarbons under conditions of smooth sliding, i.e., at velocities above the critical stick slip to smooth sliding transition velocity V_c [23]. Once movement of the lower surface is initiated, the deflection of the friction force measuring spring increases linearly with time as the upper surface moves together with the lower surface until the ''static'' friction force, F_s, is reached. This force, which is necessary to initiate sliding, is higher than the ''kinetic'' force F_k required to continue moving in the steady state. This sequence of static-to-kinetic friction is observed after every reversal of the sliding direction, as can be observed in Fig. 1. The measured kinetic friction force F_k was found to be independent of sliding velocity V in the range 0.05–11.0 μm/s, which is similar to the behavior of other linear hydrocarbon lubricants.

Another feature of the measured friction traces which has also been observed before [23] was the presence of ''stiction'' on reversing the sliding direction (Fig. 1) and in ''stop-start'' experiments. In stop-start experiments, the moving surfaces are brought to rest for a certain time Δt before sliding is resumed. On resumption of sliding, a large static

friction force (stiction spike) precedes the smooth, steady-state sliding at $F=F_k$, but only if the waiting time at rest Δt exceeds a certain critical nucleation time, τ_c. Otherwise, if $\Delta t<\tau_c$, the friction force remains unchanged at the kinetic value, $F=F_k$, before and after the sliding is stopped. The observation of time-dependent stiction spikes in stop-start experiments is an indication of stick-slip sliding at lower sliding velocities, below the critical velocity V_c [23] (although we did not slide at very low velocities and did not observe stick-slip sliding in these experiments), and the phenomenon has been associated with a change of state of the film from a frozen solidlike state (exhibiting high frictional resistance to sliding) to a molten liquidlike state responsible for the lower kinetic friction force associated with smooth, steady-state sliding [24]. However, it has not been possible to directly observe the expected structural changes in shearing films.

After shearing the liquid film back and forth for 5.75 cycles at constant speed V, the driving motion of the lower surface was suddenly stopped at some point near the middle of the smooth (steady-state) sliding part of the cycle and, simultaneously, the heaters were turned off and liquid nitrogen was injected onto the surfaces and into the SFA chamber to quickly reduce the temperature of the system and quench the film in its steady-state sliding configuration. Quenching therefore occurred at a point P in Fig. 1. The time elapsed between the stopping of the shear and the freezing of the film was less than 5 sec, as could be observed from direct imaging of the surfaces under a microscope where the rapid appearance of hydrocarbon crystals around the contact region could be easily detected, as well from the interference fringes that became increasingly dimmer as the film solidified. Furthermore, continual monitoring of the interference fringes allowed us to be sure that the surfaces remained in flat contact, without moving apart, throughout the freezing process. The freezing time of a few seconds, while many orders of magnitude longer than any molecular relaxation time in the bulk liquid, is however short enough for the *confined* molecules that no stiction spike would have been observed if the sliding would have been resumed under the same experimental conditions. In other words, the time to freeze was less than the critical nucleation time, τ_c, which we take to indicate that the films were preserved in their liquidlike rather than their solidlike state.

After the initial freezing of the film, liquid nitrogen was periodically added to the SFA chamber for more than 20 min; during this time the temperature of the whole apparatus fell to below room temperature and was kept at 20 °C throughout each experiment (16 °C below the melting point of eicosane). This procedure was adopted to prevent any possible remelting of the confined film. As was shown by Christenson [25], a strong depression of the melting point may occur for confined hydrocarbon films between molecularly smooth mica surfaces. Thin films of *n*-eicosane, however, do not appear to remain in the liquid state at temperatures more than 10 °C below the melting point [25]. After finishing the addition of liquid nitrogen and allowing the temperature of the whole SFA to reach 20 °C the mica surfaces were separated from each other by applying a tensile strain using the normal loading-unloading spring mechanism of the SFA-III. Once a certain tension was applied to the surfaces, they suddenly jumped apart, fracturing (splitting) the hydrocarbon film either within the 1.5-nm-thick film or at one of the two film-mica interfaces.

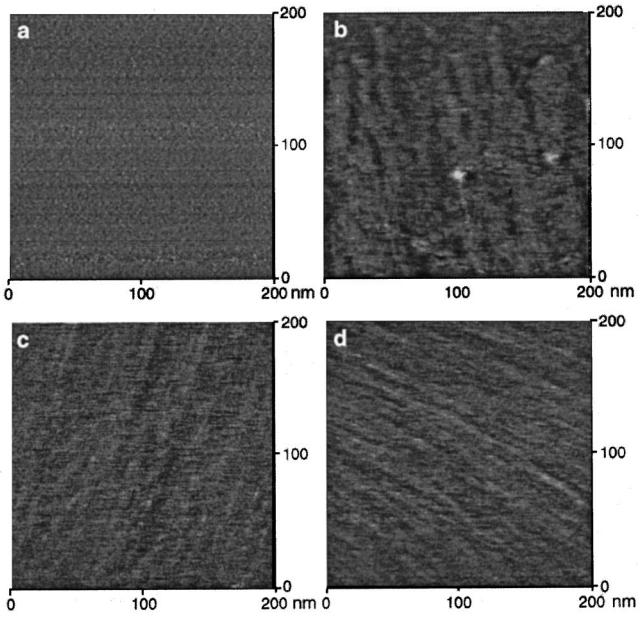

FIG. 2. Tapping mode AFM phase images of confined *n*-eicosane films after freezing and fracturing as described in the text. The range of the phase is 7° for all the images, and scanning was in the left-right (horizontal) direction. (a): Film not subjected to shear. (b): Film sheared in the vertical direction at $V=0.55\ \mu$m/sec before freezing. (c) and (d): Differently located films sheared in the vertical direction at $V=5.6\ \mu$m/sec before freezing. The height scale of the corresponding height images is 4 Å, and the height of the observed strips is between 1 and 2 Å. Films (b)–(d) were sheared in the vertical direction. The preparation and treatment of the surfaces (besides the application of the shear) and the imaging conditions were identical for all the samples. No aging effects were detected even after storing the samples in vacuum at 4°C for 1 year. All scans were performed at 20°C.

The surfaces were then removed from the SFA chamber. By visual inspection, it was clear that the frozen hydrocarbon material was mostly present on only one of the two mica surfaces, with an apparently equal probability of remaining on the upper or lower surface in different experiments. In all, four different experiments were performed between surfaces under identical conditions (except that their relative crystallographic orientations or lattice ''twist angles'' were not controlled) at different sliding speeds. AFM images of the surfaces at the contact spots were obtained and are presented in Fig. 2. The presence of bulk hydrocarbon around the contact region made it easy to find their exact locations using an optical microscope attached to the AFM. The AFM scans were taken at 20–22 °C with a Dimension 3000 Scanning Probe Microscope (Digital Instruments) in tapping mode, at a scan rate of 2.04 Hz and very low load to avoid remelting or deformation of the film [26]. Etched silicon probes with nominal tip radii of 5–10 nm and force constants in the range 20–80 N/m were used. These tips had a thickness, mean width, and cantilever length of 4, 30, and 125 μm, respec-

tively, and a resonance frequency of ~330 kHz. Even though these tips were too large to achieve molecular resolution, they allowed us to determine the existence of longer-ranged ordering/structuring on or within the shearing films. To achieve even better resolution, we also looked at some of the surfaces with high-resolution supersharp ''SC Super Cone IBM'' tapping-mode AFM tips (Veeco) with a rated tip radius of 2–5 nm (instead of ~10 nm). The resulting high-resolution images of two different but representative stripes are shown in Figs. 3(a) and 3(b), showing them to have a width of ~3.0 nm, and a height of ~0.2 nm. However, any *molecular-scale* organization within the stripes could still not be established even from these high-resolution images. This could be due to the difficulty of obtaining images with molecular resolution of this soft material.

We also studied films that were prepared and treated in exactly the same way as described above, only *without* applying any shear to them. This was done to distinguish between the effects of shear and confinement on the structure of the confined films. To see whether the films ''aged'' with time, AFM images were also taken 1 day, 1 week, and 1 year after each experiment, without any noticeable difference: Prior to and after each imaging the surfaces were stored in vacuum at 4 °C. On the other hand, once the samples were heated from 4 to 31 °C for 1 h, the resulting AFM images [Figs. 3(c) and 3(d)] show that the two-dimensional (2D) stripes melt and ''round-up'' into small droplet lens on the surfaces, which is analogous to the ''balling-up'' of a liquid filament in 3D.

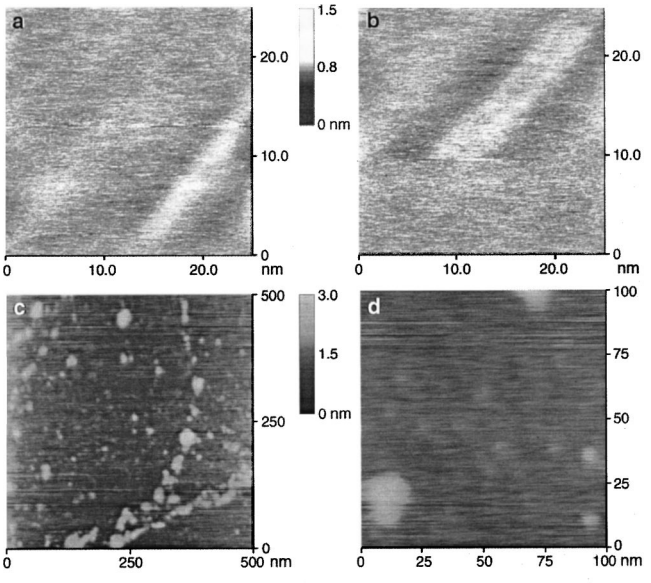

FIG. 3. (a) and (b): High-resolution tapping mode AFM height images using ultrasharp tips of two different stripes as in Fig. 2. (c) and (d): Images of surface films as in Fig. 2 after heating to 31°C (similar images were obtained when scanned at 31°C or after resolidifying to 20°C). The surfaces of the islands or lenses were rounded (convex) with a maximum height at their center of about 1.5 nm; this may be compared to the uniform height (thickness) of ~0.2 nm of the stripes from which they were formed.

IV. DISCUSSION AND CONCLUSIONS

The AFM images of Fig. 2 provide clear evidence of velocity-dependent structural changes in the confined films due to shear. There is no sign of any preferred alignment induced by *confinement only* [Fig. 2(a)], but clear signs of elongated domains in similarly confined shearing films are present. The long oriented stripes seen in Figs. 2 and 3 are typically 1–2 Å high, a few nanometers wide, and some tens of nanometers long. At higher velocities the lines were systematically sharper, narrower, and longer, as shown in Figs. 2(c) and 2(d). The results seem to indicate an increase in the long-range order with increasing shear rate for the same sliding distance sheared.

These relatively long-lived structures are consistent with the tribological results, such as those obtained from the stop-start experiments [23], which show that confined films take a long time—of the order of tens of seconds or more—to change their state; for example, to transform from the liquidlike state to the solidlike state, and even longer to return to the original unsheared amorphous state. Interestingly, these results suggest that what has traditionally been called the liquidlike, low friction state actually corresponds to a state that displays (shear-induced) long-range structural order.

The results of Fig. 2 further show that the *n*-alkane molecules order into discrete layers under both shearing and static conditions. This is evident from the smoothness (uniform thickness to ±1 Å) of different regions or patches of the surfaces. This is also consistent with previous experiments on the adsorption of *n*-alkanes on mica [27], Au(100) [28], Au(111) [29], Pt(111) [30], Ag(111) [31], and graphite [32], which have invariably shown that these linear molecules adsorb in the form of discrete layers in which the molecules lie parallel to the surfaces, but are not necessarily ordered within each layer. In our experiments the confined films of mean thickness ~15 Å consisted of ~4 molecular layers sandwiched between two mica surfaces whose surface crystallographic axes were oriented at random. Studies with perfectly aligned (commensurate) mica lattices may produce different results due to the cooperative epitaxial ordering imposed on the confined molecules. Some molecular dynamics simulations of hydrocarbon films between highly confined structured surfaces have found layering, but only short-range order within each layer, under static conditions [33], which are largely unaffected by shear [19]. In contrast, other studies covering larger shearing distances [16–18] found significant shear-induced ordering into layers and alignment within each layer. The results of computer simulations are therefore still somewhat equivocal and, as mentioned before, these simulations cover very small sliding distances (or strains) and short shearing times compared to those covered in the experiments. It has been experimentally established that the distance sheared has a large effect on the shear-induced ordering and friction forces in thin films [20]. Our failure to observe molecular-level ordering within the striped shear-induced domains even when scanned with fine AFM tips may be due to the softness of these surfaces or to the existence of only short-range order. However, the fact that the AFM results reveal discrete layers having atomically smooth surfaces strongly suggest that there must be some order

within each layer and, based on previous friction-force experiments, that this order is different from that in unsheared films. It is most likely, therefore, that the molecules of the unsheared films, while well ordered into discrete layers, exhibit no preferred orientation or alignment within the layers (i.e., each layer is amorphous or composed of random 2D coils), while the sheared films have some additional molecular alignment within each layer or domain that may be of short range only.

As can be readily noted in Fig. 2, the stripes on the sheared surfaces are not parallel to the scan direction (from left to right) nor to the shear direction (from top to bottom) but aligned at some finite angle θ to it which, even in the same sample, appears to change with sliding velocity and location. Thus, domains oriented both clockwise and counterclockwise to the shear direction were observed in different regions of the same contact area, but no clear grain boundary between two differently oriented regions was ever observed. Changing the scan angle from 0° to 90° during the scanning of the surfaces resulted in identical images, thereby ruling out structural effects induced by the AFM tip or the scan direction. From the limited set of data obtained so far, it seems that at low sliding velocity ($V=0.05$ μm/s) the stripes are on average oriented closer to the sliding direction, with an average angle of $\theta=30°\pm5°$, compared to the highest sliding velocity investigated ($V=5$ μm/s) where the average angle was $\theta=42°\pm8°$. The quoted errors correspond to the standard deviations of the angles measured at different regions of the contact areas of several sheared samples. The variability of the orientation of the observed lines is illustrated by the AFM images of Figs. 2(c) and 2(d), which were obtained in different spots within the same contact region. These images are also typical of the highest and lowest orientation angles observed in a particular experiment.

The molecular structure of the oriented stripes or domains is open to several interpretations. As already mentioned, from the images alone, it was not possible to determine the exact orientation of the *individual molecules* within each domain (cf. Fig. 3). The widths of the domains (a few nanometers) greatly exceed the hydrocarbon molecular diameter of 0.36 nm (3.6 Å), so that they cannot be associated with individual molecules. However, they could be *bundles* of molecules, aligned either parallel or perpendicular to the domain axis, or even at some angle to it. Indeed, even-numbered alkanes in the bulk solid phase are known to adopt a lamellar (smecticlike) structure, with each molecule tilted at an angle of $\alpha=72°$ to the lamellar plane [34] as shown in Fig. 4(a). This angle can be different for adsorbed molecules: for example, for *n*-hexadecane adsorbed on Au(111) or Au(100) the tilt angles are $\alpha=60°$ [29] and $\alpha=90°$ [28], respectively. Molecular simulations on confined alkane layers between two shearing model surfaces with tethered short hydrocarbon chains by Gupta, Cochran, and Cummings [17] found that at separations where an integral number of layers exist between the surfaces, as is the case in our experiments, the molecules align along the sliding direction, and there is substantial slip at the walls with an almost planar velocity profile in the film (plug flow). Substantial wall slip was also found by Khare, de Pablo, and Yethiraj [18] in simulations of confined

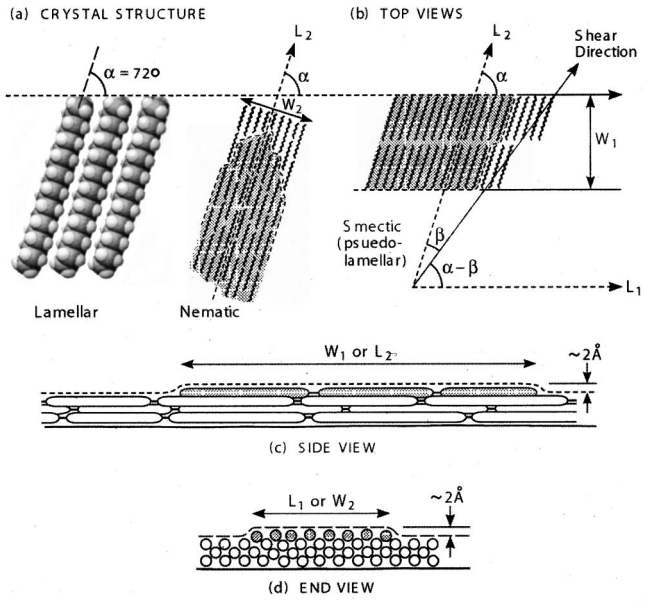

FIG. 4. (a) Bulk crystalline structure of even-chained linear hydrocarbons (adapted from [32]). The molecular backbones are parallel to each other and subtend an angle of $\alpha=72°$ to the lamellar plane. (b), (c), and (d): proposed top, side, and end views of the confined hydrocarbon films under shear where the dotted lines show the likely cleavage directions or planes when the interface is freeze fractured. The widths and lengths of the striped domains (shaded regions) are denoted by W_1, L_1 and W_2, L_2 corresponding to the two possible cleavage directions as indicated by the labeled arrows and dashed lines.

sheared linear polymers. The occurrence of wall slip, however, is likely to be determined by different factors than the film structure, such as the fine details of the liquid-solid interaction [35], although both the relative orientation of the surface lattices *and* the sliding direction are expected to play a role in determining the molecular alignment.

Given our results and those of simulations that have often been ambiguous regarding the ordering of chain molecules in sheared films [17–19], the configuration of the molecules within the shearing layers (striped domains) may be ordered over a short range only, nematic or pseudolamellar as shown in Figs. 4(b)–4(d), in which case it is reasonable to expect that the frozen film will fracture along one of the dashed lines. This model can also explain the varying and nonzero orientations of the domains observed on the AFM images relative to the sliding direction, and the ~2 Å domain heights. Thus, referring to Fig. 4(b), if the molecular backbones subtend an angle β to the shear direction (where β is determined by the sliding direction and the two surface lattice directions), the striped domains could subtend angles β or $(\alpha\text{-}\beta)$ to the shear direction, depending on the cleavage planes. It is interesting to note that for $\beta=30°$ and $\alpha=72°$ (the bulk value), we expect $\beta=30°$ and/or $(\alpha\text{-}\beta)=42°$, which agree with the *mean* value of the measured angles.

A more detailed investigation of the effects of (1) the relative crystallographic orientation of the two mica surfaces (the lattice twist angle), (2) the direction of sliding relative to (one of) these lattice axes, and (3) the sliding velocity, on the structure of confined films is currently in progress. It would

also be interesting to know how much shearing is required for a film to fully align, and then relax back to its original state after the shearing is stopped. Other experimental techniques, such as various *in situ* spectroscopic techniques may be required to obtain the full picture.

ACKNOWLEDGMENTS

This work was funded by grants from the Office of Naval Research under ONR Grant No. N00014-93-1-0269 and the W. M. Keck Foundation under Grant No. 991703.

[1] A. Berker, S. Chynoweth, U. C. Klomp, and Y. Michopoulos, J. Chem. Soc., Faraday Trans. **88**, 1719 (1992).
[2] S. T. Cui, S. A. Gupta, P. T. Cummings, and H. D. Cochran, J. Chem. Phys. **105**, 1214 (1996).
[3] L. I. Kioupis and E. J. Maginn, Chem. Eng. J. (Lausanne) **74**, 129 (1999).
[4] J. D. Moore, S. T. Cui, H. D. Cochran, and P. T. Cummings, J. Non-Newtonian Fluid Mech. **93**, 83 (2000).
[5] C. Riekel, in *Neutron, X-Ray, and Light Scattering: Introduction to an Investigative Tool for Colloidal and Polymeric Systems*, edited by P. Lindner and T. Zemb North-Holland Delta Series (North-Holland, Amsterdam, 1991), pp. 279–98.
[6] R. C. Oberthür, Rev. Phys. Appl. **19**, 663 (1984).
[7] *Neutron, X-Ray, and Light Scattering: Introduction to an Investigative Tool for Colloidal and Polymeric Systems*, edited by P. Lindner and T. Zemb, North-Holland Delta Series (North-Holland, Amsterdam, 1991).
[8] Y. T. Hu, P. Boltenhagen, and D. J. Pine, J. Rheol. **42**, 1185 (1998).
[9] G. Wiberg, M. L. Skytt, and U. W. Gedde, Polymer **39**, 2983 (1998).
[10] B. L. Riise, G. H. Fredrickson, R. G. Larson, and D. S. Pearson, Macromolecules **28**, 7653 (1995).
[11] P. Hébraud, F. Lequeux, J. P. Munch, and D. J. Pine, Phys. Rev. Lett. **78**, 4657 (1997).
[12] I. Koltover, S. H. J. Idziak, P. Davidson, Y. Li, C. R. Safinya, M. Ruths, S. Steinberg, and J. N. Israelachvili, J. Phys. II **6**, 893 (1996).
[13] Y. Golan, A. Martin-Herranz, Y. Li, C. R. Safinya, and J. Israelachvili, Phys. Rev. Lett. **86**, 1263 (2001).
[14] I. Soga, A. Dhinojwala, and S. Granick, Langmuir **14**, 1156 (1998).
[15] T. L. Kuhl, G. S. Smith, J. N. Israelachvili, J. Majewski, and W. Hamilton, Rev. Sci. Instrum. **72**, 1715 (2001).
[16] M. J. Stevens, M. Mondello, G. S. Grest, S. T. Cui, H. D. Cochran, and P. T. Cummings, J. Chem. Phys. **106**, 7303 (1997).
[17] S. A. Gupta, H. D. Cochran, and P. T. Cummings, J. Chem. Phys. **107**, 10 327 (1997).
[18] R. Khare, J. J. de Pablo, and A. Yethiraj, Macromolecules **29**, 7910 (1996).
[19] P. A. Thompson, M. O. Robbins, and G. S. Grest, Isr. J. Chem. **35**, 93 (1995).
[20] C. Drummond and J. Israelachvili, Macromolecules **33**, 4910 (2000).
[21] G. Luengo, F-J. Schmitt, R. Hill, and J. Israelachvili, Macromolecules **30**, 2482 (1997).
[22] A. M. Homola, J. N. Israelachvili, M. L. Gee, and P. M. McGuiggan, J. Tribol. **111**, 675 (1989).
[23] H. Yoshizawa and J. Israelachvili, J. Phys. Chem. **97**, 11 300 (1993).
[24] P. A. Thompson and M. O. Robbins, Science **250**, 792 (1990).
[25] H. K. Christensen, Phys. Rev. Lett. **74**, 4675 (1995).
[26] M. Plomp, P. J. C. M. van Hoof, and W. J. P. van Enckevort, Surf. Sci. **448**, 231 (2000).
[27] G. Valdrè, A. Allessandrini, U. Muscatello, and U. Valdrè, Philos. Mag. Lett. **78**, 255 (1998).
[28] R. Yamada and K. Uosaki, Langmuir **16**, 4413 (2000).
[29] K. Uosaki and R. Yamada, J. Am. Chem. Soc. **121**, 4090 (1999).
[30] L. E. Firment and G. A. Somorjai, J. Chem. Phys. **66**, 2901 (1977).
[31] L. E. Firment and G. A. Somorjai, J. Chem. Phys. **69**, 3940 (1978).
[32] M. S. Couto, X. Y. Liu, H. Meekes, and P. Bennema, J. Appl. Phys. **75**, 627 (1994).
[33] J. Gao, W. D. Luedtke, and U. Landman, J. Chem. Phys. **106**, 4309 (1997).
[34] I. Denicolò, J. Doucet, and A. F. Craievich, J. Chem. Phys. **78**, 1465 (1983).
[35] E. Manias, G. Hadziioannou, I. Bitsanis, and G. ten Brinke, Europhys. Lett. **24**, 99 (1993).